Stratigraphic Inversion of a Wabamun Carbonate play – Parkland Field

Rick Walia and Jennifer Melnychyn, CGG Canada Services Ltd., Calgary*

Abstract

The Famennian subsurface strata in the Western Canadian Sedimentary Basin (WCSB) consist of a series of stacked NW dipping carbonate ramps of the Wabamun group with very significant gas potential. The Parkland field was discovered in 1956 and has produced more than 100 Bcf. There are two wells on the field, about 75% of the gas production is from the first well (6-29), however the nearby second well (10-28) has contributed only ~25Bcf. This case study is an attempt to explain the anomalous production behaviour over such a short distance, ~2km.

Introduction

The Parkland Wabamun A gas pool, in the Peace River Block of NE British Columbia (TWP 81 RGE 15 W6M), was discovered in 1956 (Fig. 1). This pool has an in-place-volume of over 225Bcf of which more than 100Bcf have already been produced. Production is from porous Devonian Wabamun carbonates at a depth of ~3300m. Porosity is well defined in two wells, 10-28 and 6-29. The porous Wabamun carbonates at the well 10-28 have a sonic P wave velocity of about 4200 m/s, while the velocity of the surrounding tight Wabamun carbonates is about 5500 m/s.

Seismic data Processing

CGG acquired the Parkland 3D seismic data as a group shoot over a 16 sq. km area with a bin size of 35 x 35m. Four Vibrators were used as the seismic source. The data was originally processed in 1991 with a simple processing flow, which included: *True amplitude gain recovery, instrument and geophone phase corrections, deconvolution, 3D weathering statics and 3D surface consistent statics, 3D DMO and one pass 3D FX migration*. Fig.2b shows one EW line where this processing flow was used.

Interpretative Stratigraphic Processing

For the inversion work, the seismic data was reprocessed with a high-resolution amplitude preserving flow which included the following special steps: *3D Interactive geometry QC (SDITR), 3D surface consistent spiking deconvolution, 3D weathering and elevation statics, 3D surface consistent autostatics, a high-resolution 3D DMO, 3D FX migration and FX noise elimination projection filter (SPARN).* Log data from the well 10-28 was used to derive a match filter for stratigraphic deconvolution to finally zero-phase the data, and to restore low as well as higher frequencies. Fig.2 compares a section from this flow with the previous processing.

3D Stratigraphic Inversion – Methodology

The inversion method, called TDROV, describes the existing zero-phase 3D volume by a discrete number of impedance layers. Each layer consists of a time, thickness, and impedance value at every bin location. Convergence to the final solution is achieved using a full 3D algorithm based on simulated annealing (*Gluck et al., 1997, Duboz, 1998*). The following three features of this new inversion method are particularly noteworthy.

1. **Well logs are not input to the inversion process:** Most inversion schemes would steer an inverted AI (Acoustic impedance) trace to match the impedance log at the well locations. Certain zones on the synthetic trace may not match the seismic or VSP data. There could be several reasons for such a mismatch e.g., wash-out zone, mud-cake build-ups & micro-scale (a few cm) resolution of the logs, and multiples, processing artifacts and mega-scale resolution (a few hundred meters spatial & a few meters vertical) of the seismic data. Therefore, over-influencing the inversion process with the log data is not an optimal solution. Another disadvantage of such a *forced-match* is that we lose the opportunity to investigate any problem with the log or seismic data. On the other hand, because this inversion honours seismic data, any mismatch between the AI trace and the impedance log data would suggest that there could be problem with either the log or seismic data.

2. **Resolution and tuning effects:** This inversion scheme is constrained by the stratigraphy, which is input through the seismic horizon picks. It builds thin layers between the seismic picks to create an initial thin-layer model. The initial thickness of the thin layers interpolated between the seismic picks depends on the seismic frequency bandwidth and on the formation thickness on the logs. The initial model parameters are perturbed in reflection time and impedance to yield a unique solution. This approach leads to improved resolution while eliminating tuning effects *(Walia et. al., 1999, Scott et. al., 2000).*

3. **Uniqueness of inversion results:** This inversion scheme employs a 3D algorithm and uses a thin layer model, as discussed above. The seismic response of the impedance model is compared with the seismic data in a volumetric fashion by measuring the error along the mobile impedance model interfaces. The resulting misfit is minimized in order to maximize the probability function of the impedance model parameters. In doing so, the impedance model interfaces tend to orient themselves conformably to the seismic reflectors, thereby averaging out the random noise, and reinforcing laterally weak but coherent events and a global minimum is achieved.

Inversion results

The initial model input to the inversion process consisted of five seismic horizon picks namely, Bluesky, Nordegg, Belloy, Debolt and Wabamun that defined the stratigraphy. No log data was input explicitly to the inversion process. A proportional type of geometry was defined to create thin layers within the initial model. The initial thickness of these thin layers was ~6ms based on the frequency bandwidth available in the seismic data. Fig.3 displays the inversion results within the reservoir zone. The thick yellow line in the middle is the low-frequency initial impedance and the shaded yellow area is the impedance corridor defined in the initial model. To verify the inversion results, the impedance log from the well 10-28 is pasted in black under the red inverted impedance trace, no impedance log is available for the well 6-29. An excellent agreement between the impedance log of the well 10-28 and the inverted trace at the well location clearly points out that the thin layers 177 to 181 constitute the reservoir.

Reservoir layers 177-181 are in a time interval which is about 25ms and corresponds to a depth of ~3260-3310m, which means this inversion process has resolved layers with average thickness of ~12m for this seismic data. A seismic line passing through the well 6-29 and a corresponding impedance section are shown in Fig.4. Layer 176 (shown in black on the impedance section, ~1550ms) corresponds to the top of Wabamun pick and as expected a higher impedance value (red) due to low porosity carbonates can be seen. However, the amplitude anomaly that is seen in the seismic data at ~1580ms, has been inverted as three low impedance thin layers (shown in blue) corresponding to gas charged dolomitized carbonates. Also, below these blue layers we see two thin green layers followed below by the high impedance (red) layers corresponding to the low porosity Wabamun carbonates.

Fig.5 compares the impedance profiles through the wells 10-28 and 6-29 in terms of number of layers and their impedance values. It is clear that there are only two reservoir layers around the well 10-28 versus almost four to five thin layers at the well 6-29. Additionally the impedance values are lower around 6-29 suggesting higher porosity and/or higher gas effect. Also, a typical collapsed feature present around 6-29 is indicative of better facies. Factors discussed above clearly demonstrate that the producing reservoir zone around the well 6-29 is superior in facies quality and also thicker than the producing zone at the well 10-28. From the comparison of the layer maps corresponding to the reservoir tops at 10-28 (layer177) and 6-29 (layer 178), shown in Fig.6, it can be concluded that layer 177 has good facies (low impedance ~12000 m/s gm/cc) at 10-28. However, layer 178 is much better (in terms of even lower range of impedance values ~10,000 m/s gm/cc) around 6-29. It suggests that there is a significant lateral variation in impedance values within these thin layers. For example, layer 178 has low impedance values in the EW and NS directions around the well 6-29, but the impedance values become higher in an eastwardly direction as it approaches well 10-28, closer to the main fault. Fig.7 shows layer maps of the next two layers, which clearly suggest that there is a desirable range of impedance values centered at the well 6-29. The impedance values within these layers at 10-28 correspond to that of background tight limestone. In general, except for layer 177, the impedance value increases as the main fault is approached, either eastward or northward, exhibiting a relationship between the dolomitization process versus the distance from the main fault (which at one time acted as conduit for hot brine fluids that have caused the dolomitization).

Conclusions

The case study presented here clearly demonstrates the advantages of using a layered impedance cube to improve seismic interpretation. The automatic identification of the thin layer geometry conforms to the geological strata, improves seismic interpretation and helps in identifying features not evident in the seismic data alone. These impedance layers are directly correlatable with the log data at the well locations. This provides extremely important, but otherwise missing, information about the lateral and vertical impedance variation between the wells. As discussed, the inversion process resolved four thin layers of low-impedance (indicating good porosity) around well 6-29 while only two thin layers were mapped around the well 10-28, thereby providing an explanation for the significant difference in production from the two wells. Also, a much clearer definition of a collapsed feature, indicative of better porosity development, around the well 6-29 can be seen in the impedance sections.

Acknowledgements

I am grateful to Todd Mojesky for all his guidance and supervision in data processing and inversion work. My sincere thanks to Dave Richert for supplying horizon picks and other geological data for this case study. I thank Steve Raleigh and Radim Vesely for the internal review and suggestions. I am also thankful to CGG for the permission to publish the results.

References

Duboz, P, Y. Lafet and D. Mougenot, Moving to a layered impedance cube: advantages of 3D stratigraphic inversion, First Break, Sept. 1998, pp311-318.

Gluck, S., E. Juve and Y. Lafet, High-resolution impedance layering through 3-D stratigraphic inversion of the poststack seismic data, The Leading Edge, Sept 1997, pp1309-1315.

Scott, D., Boyle, P., Walia, R. and Mojesky, T., Identifying internal flow barriers in the Wayne oil field using a full 3-D inversion, Presented at GeoCanada 2000 held in Calgary, May29-June2, 2000.

Walia, R., Mojesky, T., Sydora, L. and Evans, J., Mapping of thin reservoir layers within the Hibernia formation using a full 3-D stratigraphic inversion, Expanded Abstracts, Vol.1, SEG 69th Ann. Mtg., 1999, pp915-918.

Figures

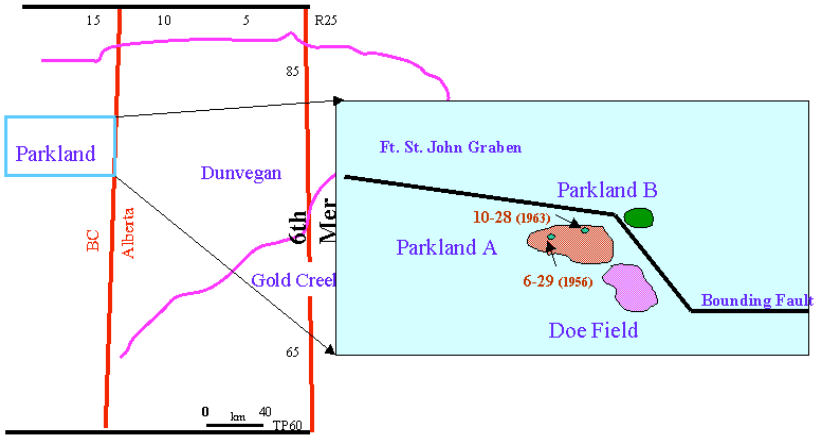

Figure 1: Map of the area showing Parkland and nearby Wabamun Pools.

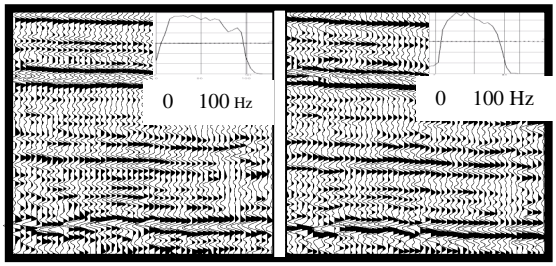

(a) Interpretive Stratigraphic Processing *(b) Structural Processing*

Figure 2: Comparison of old and new processing. (a) For high resolution inversion work an amplitude preserving processing flow was carried out, which included a surface consistent decon, FX projection noise elimination filter, another surface consistent phase decon, a high resolution DMO, post-stack migration, spectral whitening and a stratigraphic decon to zero phase the data based on log data. (b) The older processing followed a simple processing flow, which included a shot decon, statics, DMO and a migration.

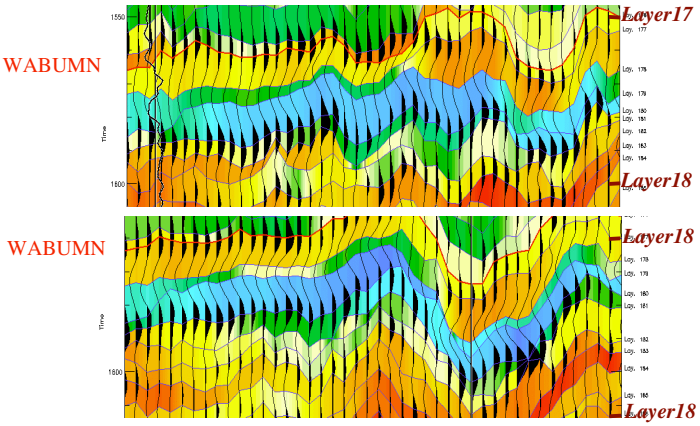

Figure 5: Seismic data superimposed on the impedance section. TDROV provides the identification of thin reservoir layers along with the vertical and lateral variations of the absolute AI in each layer.

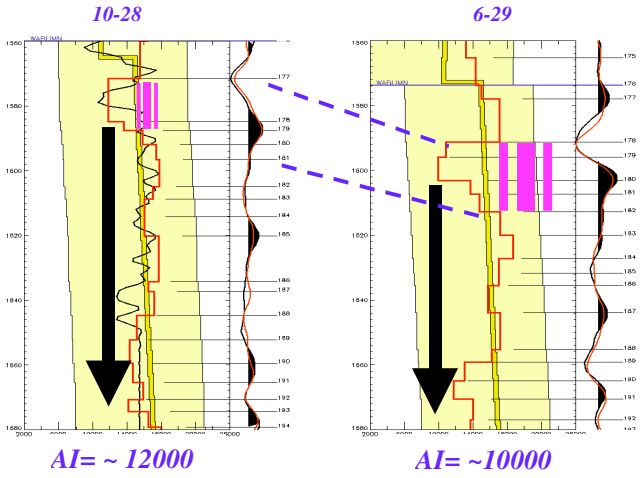

Figure 3: To QC inversion results inverted impedance trace is superimposed on the impedance log. The reservoir is now defined in terms of 6 micro layers (layer 177-182). The total thickness and the AI values of the reservoir layers match both the log and production data. The AI within each micro layer can now be mapped for the whole volume.

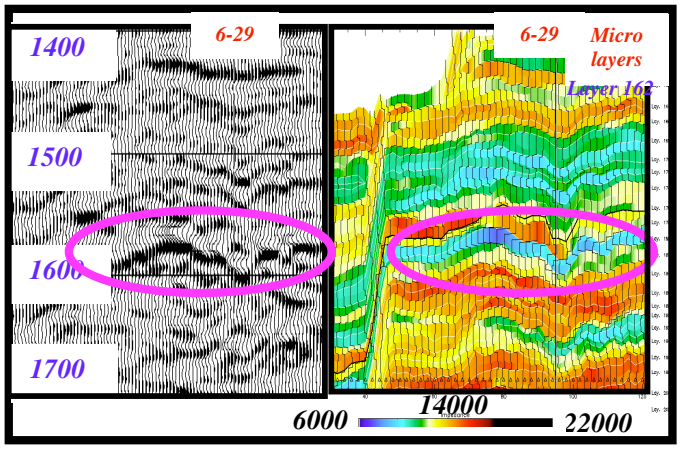

Figure 4: Seismic versus the inverted impedance section. Note excellent details of the collapse structure (main play in the Parkland A pool) along with lateral and vertical variations of AI within each micro layer. Blue colour indicates low AI or high porosity reservoir layers. High porosities of thin dolomitized layers in the Parkland play have been precisely delineated.

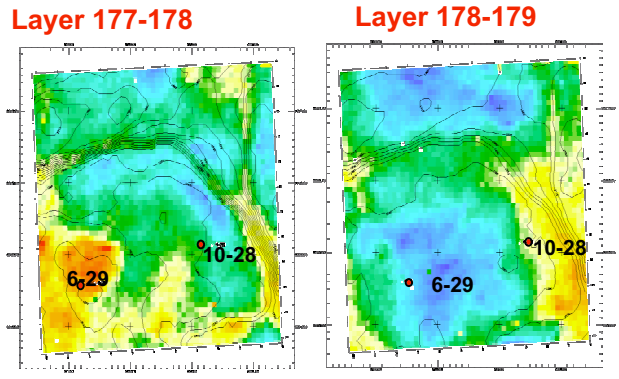

Figure 6: Thin reservoir layers and the AI variation can be mapped over the field. In this case, TDROV interpreted 208 layers over a time window of ~1200ms. Five layers were identified within the gas reservoir (layers 177-181). Blue/green show a range of low AI values corresponding to good reservoir porosities. These maps can be used to place producer/injector well locations.

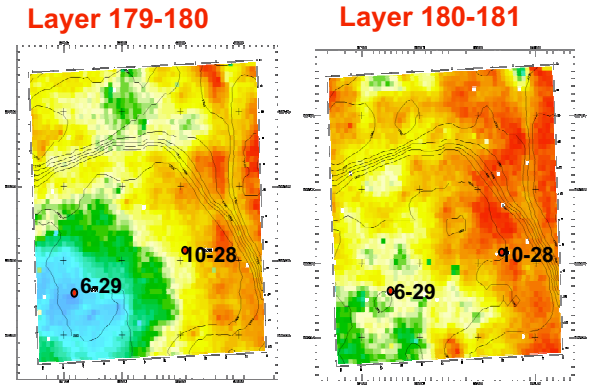

Figure 7: Maps of the next two reservoir layers. Good quality reservoir facies around the well 6-29 (as shown by these maps) clearly explains that why well 6-29 has produced almost four times more than the nearby well 10-28.